

GAMMA-RAY FLARES FROM RED GIANT/JET INTERACTIONS IN AGN

MAXIM V. BARKOV^{1,2}, FELIX A. AHARONIAN^{1,3} AND VALENTÍ BOSCH-RAMON¹

¹Max-Planck-Institut für Kernphysik, Saupfercheckweg 1, 69117 Heidelberg, Germany

²Space Research Institute, 84/32 Profsoyuznaya Street, Moscow, 117997, Russia

³Dublin Institute for Advanced Studies, 31 Fitzwilliam Place, Dublin 2, Ireland

Draft version October 27, 2018

ABSTRACT

Non-blazar AGN have been recently established as a class of gamma-ray sources. M87, a nearby representative of this class, show fast TeV variability on timescales of a few days. We suggest a scenario of flare gamma-ray emission in non-blazar AGN based on a red giant interacting with the jet at the base. We solve the hydrodynamical equations that describe the evolution of the envelope of a red giant blown by the impact of the jet. If the red giant is at least slightly tidally disrupted by the supermassive black hole, enough stellar material will be blown by the jet, expanding quickly until a significant part of the jet is shocked. This process can render suitable conditions for energy dissipation and proton acceleration, which could explain the detected day-scale TeV flares from M87 via proton-proton collisions. Since the produced radiation would be unbeamed, such an events should be mostly detected from non-blazar AGN. They may be frequent phenomena, detectable in the GeV-TeV range even up to distances of ~ 1 Gpc for the most powerful jets. The counterparts at lower energies are expected to be not too bright. M87, and nearby non-blazar AGN in general, can be fast variable sources of gamma-rays through red giant/jet interactions.

Subject headings: active galactic nuclei: jets – TeV photons: variability – stars: red giant

1. INTRODUCTION

Active galactic nuclei (AGN) are believed to be powered by an accreting supermassive black hole (SMBH) in the center of a galaxy, a significant fraction of AGN show powerful jets, supersonic relativistic flows, on small (sub parsec) and large (multi hundred kpc) scales. (e.g. Begelman et al. 1984). These AGN are characterized by nonthermal emission extending from radio to high energy gamma-rays. This radiation comes from an accretion disc and from two relativistic jets that are launched close to the SMBH in two opposite directions. The emission associated to the accretion process can be generated by thermal plasma in the form of an optically-thick disc under efficient cooling (e.g., Shakura 1972; Shakura & Sunyaev 1973), or as an optically-thin corona (e.g., Bisnovatyi-Kogan & Blinnikov 1977; Liang & Thompson 1979). The emission from the jets is non thermal and comes from a population of relativistic particles accelerated for instance in strong shocks, although other scenarios are possible as well (see, e.g., Schopper et al. 1998; Neronov & Aharonian 2007; Rieger et al. 2007; Rieger & Aharonian 2008). This non-thermal emission is thought to be produced through synchrotron and inverse Compton (IC) processes (e.g. Ghisellini et al. 1985), although hadronic models have been also considered in the past (e.g., Mannheim 1993; Aharonian 2000; Mücke & Protheroe 2001; Aharonian 2002).

The existence of a stellar clustering in the central regions of AGN, possibly down to very small distances from the central SMBH (e.g. Penston 1988), implies that the interaction between a star and the jet should eventually happen. The gamma-ray production due to the interaction between an obstacle and an AGN jet has been studied in a number of works. For instance, Dar & Laor (1997) suggested the high-energy radiation produced by a beam of relativistic protons impacting with a cloud of the broad-line region (BLR). The gamma-ray emis-

sion from one or many clouds from the BLR interacting with a hydrodynamical jet recently has been analyzed by Araudo et al. (2010). The radiation from the interaction between a massive star and an AGN jet was studied in Bednarek & Protheroe (1997). Namely they suggested that the jet interacts with stellar winds of massive stars, in their model they assume that the source of gamma-rays is moving with a relativistic speed, therefore the radiation is Doppler boosted. The main radiation mechanism in this scenario is related to the development of the pair cascade in the field of the radiation of the massive star.

In this work, we study the interaction of a red giant (RG) star with the base of the jet in AGN and their observable consequences in gamma rays. We focus here on the case of M87, a nearby non-blazar AGN that presents very high-energy recurrent activity with variability timescales of few days (Aharonian et al. 2006; Albert et al. 2008; Acciari et al. 2009, 2010). In the framework presented here, the jet impacts the RG envelope, already partially tidally disrupted by the gravitational field of the central SMBH. The RG envelope is blown up, forming a cloud of gas accelerated and heated by jet pressure. The jet base is likely strongly magnetized (e.g., Komissarov et al. 2007; Barkov & Komissarov 2008). The jet flow affected by the impact with the RG envelope can be a suitable region for particle acceleration, and a significant fraction of the involved magnetic and kinetic energy of the jet can be transferred to protons and electrons. Although electrons may not be able to reach TeV emitting energies because of the expected large magnetic fields, protons would not suffer from this constraint. These protons could reach the star blown material, and optically-thick proton-proton (pp) interactions could lead to significant gamma-ray production in the early stages of the cloud expansion. Unlike in Bednarek & Protheroe (1997), we deal with solar-mass-type stars instead of the more rare high-mass stars, study the RG atmosphere-jet

interaction, and follow the hydrodynamical evolution of the cloud. Finally, we do not introduce any beaming factor to the radiation, since in our scenario most of the emission is produced when the cloud has not been significantly accelerated, Doppler boosting being therefore negligible.

2. THE MODEL

Main sequence stars are too compact to be significantly affected by tidal forces from the SMBH, unlike RGs, whose external layers are far less gravitationally bounded to the stellar core. Therefore, in the vicinity of a SMBH, the external layers of an RG will suffer significant tidal disruption (see Khokhlov et al. 1993b,a; Diener et al. 1997; Ayal et al. 2000; Ivanov et al. 2003; Lodato et al. 2009), which can unbound from the stellar core a cloud with significant mass $\gtrsim 10^{30}$ g. Therefore, if an RG penetrates into the innermost region of the jet, the RG envelope can be already weakly gravitationally attached to the star due to tidal disruption. In this situation, the external layers of the star can be lost due to jet ablation, which is unlikely in the case of undisrupted RGs (except for very powerful jets).

The tidal forces are important when the distance between the SMBH and the star is similar to or smaller than the tidal distance (z_T) for a given RG radius (R_{RG}) and mass (M_{RG}), where:

$$z_T = R_{\text{RG}} \left(\frac{M_{\text{BH}}}{M_{\text{RG}}} \right)^{1/3}, \quad (1)$$

and M_{BH} is the mass of the SMBH. Therefore, for a given RG-jet interaction distance to the SMBH z , the RG can lose the atmosphere layers beyond $R_{*\text{T}}$. For the case of M87, with $M_{\text{BH}} = (6.4 \pm 0.5) \times 10^9 M_\odot$ (Gebhardt & Thomas 2009), one obtains:

$$R_{\text{RG}}^{\text{T}} = z \left(\frac{M_{\text{RG}}}{M_{\text{BH}}} \right)^{1/3} \approx 76 M_{\text{RG}\odot}^{1/3} R_\odot \approx 5.3 \times 10^{12} M_{\text{RG}\odot}^{1/3} \text{ cm}, \quad (2)$$

where $M_{\text{RG}\odot} \equiv M_{\text{RG}}/1 M_\odot$. Since a solar-mass RG, the most common one, can have up to few hundreds of R_\odot , a significant fraction of the star envelope can be carried away by the jet flow up to $z \lesssim 10^{17}$ cm. Note that evidence for the presence of a radio jet has been found from M87 within a distance of $\sim 10^{17}$ cm from the SMBH (Junor et al. 1999).

The M87 TeV lightcurve obtained by Aharonian et al. (2006) shows several peaks, and each of these peaks in our model correspond to different RG-jet events. Note however that some nearby peaks may correspond to a complex disruption process, motivated for instance by a very disrupted and massive envelope, or by jet inhomogeneities. Also, it cannot be discarded that a cluster of several RGs could also enter the jet.

The time needed by the RG to cross the jet cannot be shorter than the typical M87 event duration, $t_e \sim 2 \times 10^5$ s. It cannot be longer either, since then the event duration would also be longer if there is available RG matter for removal, as expected at $z \lesssim z_T$. Therefore, $t_{\text{jc}} = t_e$, and the interaction height can be derived taking the velocity of the RG orbiting the SMBH as the

Keplerian velocity:

$$z_{\text{jc}} = \left[G M_{\text{BH}} \left(\frac{t_{\text{jc}}}{2\theta} \right)^2 \right]^{1/3} \approx 10^{16} \theta_{-1}^{-2/3} \text{ cm}, \quad (3)$$

where $\theta_{-1} = \theta/0.1$ is the jet semi-opening angle in radians. An important parameter is the power of the jet $L_j \approx 1 - 5 \times 10^{44}$ erg s $^{-1}$ (Owen et al. 2000), which we fix to $L_j \approx 2 \times 10^{44}$ erg s $^{-1}$. From L_j and the jet width, $z_{\text{jc}}\theta$, we can derive the jet energy flux at the interaction height:

$$F_j = \frac{L_j}{\pi z_{\text{jc}}^2 \theta^2} \approx 10^{14} \text{ erg cm}^{-2} \text{ s}^{-1}. \quad (4)$$

There are two regimes for the RG tidal disruption: under strong tidal interaction ($R_{\text{RG}} > R_{*\text{T}}$), the RG envelope suffers an elongation along the direction of motion of the star (Khokhlov et al. 1993a); under weak tidal interaction ($R_{\text{RG}} \sim R_{*\text{T}}$), the envelope is still roughly spherical (Khokhlov et al. 1993b). In both situations, the outer layers of the star will be swept away by the jet, forming a cloud that will quickly heat up and expand. We study the time evolution of the cloud adopting a very simplified hydrodynamical model for the cloud expansion. The heating of the cloud is caused by the propagation of shock waves, which are formed by the pressure exerted by the jet from below. Therefore, the cloud pressure is taken similar to the jet pressure (regardless it is of kinetic or magnetic nature):

$$p_j = \frac{F_j}{c} \approx p_c \approx (\hat{\gamma} - 1) e_c, \quad (5)$$

where c is the speed of light, and $\hat{\gamma}$ the adiabatic index ($\hat{\gamma} = 4/3$). The cloud expands at its sound speed (c_s), since the lateral and top external pressures are much smaller than the jet bottom one. When the cloud has significantly expanded, its pressure becomes smaller than the jet pressure from below. At that point new shocks leading to further cloud heating. We illustrate in Fig. 1, for the simplest case of weak disruption, how the spherical cloud evolves under the effect of jet pressure as seen in the plane perpendicular to the jet axis.

2.1. Weak tidal interaction (spherical case)

The system of equations that characterizes the weak tidal interaction case can be written as follows:

$$E_c = e_c \frac{4\pi r_c^3}{3} = \frac{4\pi F_j r_c^3}{3(\hat{\gamma} - 1)c} \quad (6)$$

$$\frac{dr_c}{dt} = c_s = \left(\frac{\hat{\gamma}(\hat{\gamma} - 1)E_c}{M_c} \right)^{1/2} \quad (7)$$

$$\frac{d^2 z_c}{dt^2} = \frac{\pi F_j r_c^2}{c M_c}, \quad (8)$$

where r_c and M_c are the cloud radius and mass, respectively.

The solutions to Eqs. (6-8) are:

$$r_c(t) = \frac{r_{c0}}{(1 - t/t_{ce})^2} \quad (9)$$

$$v_r(t) = \frac{2r_{c0}}{t_{ce}(1 - t/t_{ce})^3}, \quad (10)$$

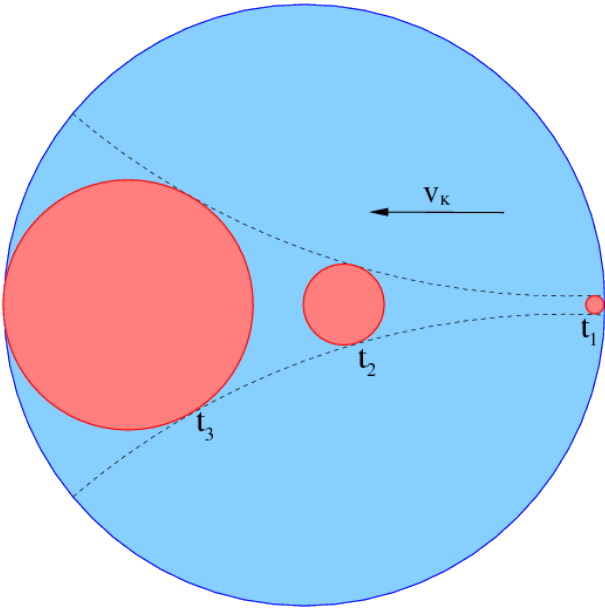


FIG. 1.— Sketch of the evolution within the jet of the cloud formed by the disrupted envelope of the RG. The plane of the image would be the jet section.

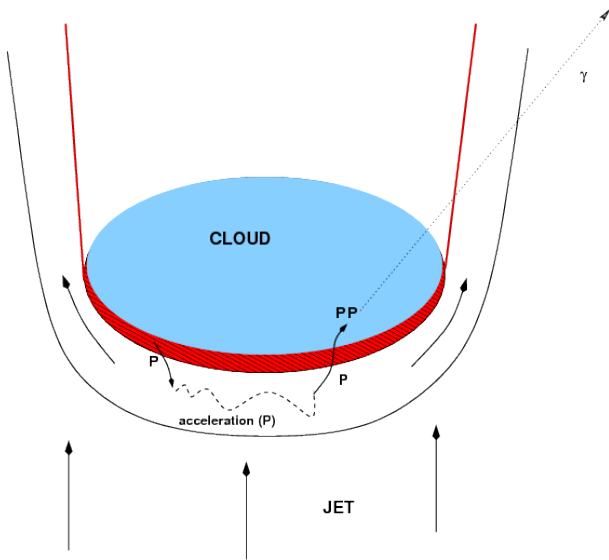


FIG. 2.— Sketch of the proton acceleration and gamma-ray production processes. The plane of the image would be normal to the jet section.

where r_{c0} , assumed to be similar to R_{*T} , is the initial cloud radius, and t_{ce} the cloud characteristic expansion time:

$$t_{ce} = \left(\frac{3cM_c}{\pi\hat{\gamma}F_j r_{c0}} \right)^{1/2} \approx 5 \times 10^5 (M_{c28}/F_{j,14} r_{c0,13})^{1/2} \text{ s}, \quad (11)$$

where $M_{c28} = M_c/10^{28}$ g. Neglecting the initial cloud velocity in the z -direction, we obtain:

$$z(t) - z_{jc} = \frac{r_{c0}}{2\hat{\gamma}} \left(\frac{t}{t_{ce}} \right)^2 \frac{3/2 - t/t_{ce}}{(1 - t/t_{ce})^2} \quad (12)$$

$$v_z(t) = \frac{r_{c0}}{\hat{\gamma}t_{ce}} \frac{(t/t_{ce})^2((t/t_{ce})^2 - 3t/t_{ce} + 3)}{(1 - t/t_{ce})^3} \quad (13)$$

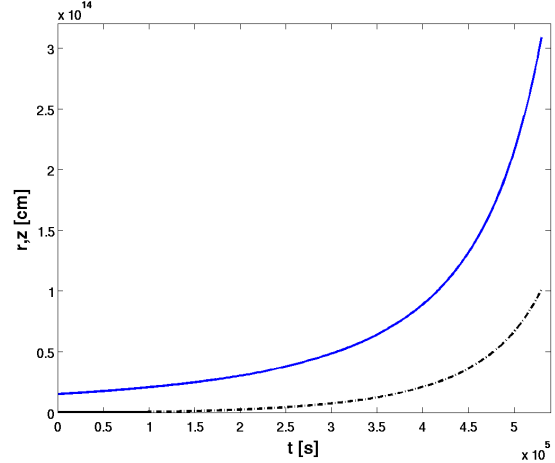


FIG. 3.— Evolution of r_c (solid line) and $z - z_{jc}$ (dot-dashed line) with time in the weak tidal interaction case. The parameter values are characteristic of M87: $L_j = 2 \times 10^{44}$ erg s $^{-1}$, $M_{BH} = 6.4 \times 10^9 M_\odot$, $\theta_{-1} = 0.5$, $M_{RG} = 1 M_\odot$, $z_{jc} \approx 2.5 \times 10^{16}$ cm, and $M_c \approx 1.3 \times 10^{28}$ gr.

where z_{jc} is the RG-jet penetration height. The evolution of the cloud radius is presented in Fig. 3. The adopted parameter values are: $L_j = 2 \times 10^{44}$ erg s $^{-1}$, $M_{BH} = 6.4 \times 10^9 M_\odot$, $\theta_{-1} = 0.5$, $M_{RG} = 1 M_\odot$, $z_{jc} \approx 2.5 \times 10^{16}$ cm, $M_c \approx 1.3 \times 10^{28}$ gr. Note that for times $t < t_{ce}$, $z - z_{jc} \ll r_c < \theta z_{jc}$ and $v_z \ll c_s \ll c$.

Making the cloud and jet pressures comparable, the energy transfer can be overestimated beyond a certain radius (r_{ct}) and time (t_t) during the cloud evolution, in which energy balance is to be fulfilled:

$$\frac{dE_c}{dt} \leq \pi r_c^2 F_j. \quad (14)$$

Using Eqs. (9) and (10), (14) permits to derive t_t :

$$t_t = t_{ce} \left(1 - \frac{8}{\hat{\gamma} - 1} \frac{r_{c0}}{t_{ce} c} \right). \quad (15)$$

Substituting Eq. (15) into Eq. (9), we obtain r_{ct} :

$$r_{ct} = \frac{r_{c0}}{\left(\frac{8}{\hat{\gamma} - 1} \frac{r_{c0}}{t_{ce} c} \right)^{2/3}} \approx 1.5 \times 10^{14} M_{c,28}^{1/3} F_{j,14}^{-1/3} \text{ cm}. \quad (16)$$

Thus, if $r_c < r_{ct}$, the solutions presented in Eqs. (6)–(8) are valid. After t_t , $dE_c/dt \sim \pi r_c^2 F_j$ yields a slower increase of r_c with t , although this should be still a fast exponential growth. We consider $t < t_t$ since we focus here on the case when the cloud is optically thick to pp collisions (see below), and at $t > t_t$ the cloud density is already too low.

2.1.1. Strong tidal interaction (elongated case)

In the case of strong tidal interaction the RG atmosphere is stretched in the direction of motion of the star, and the expansion will be now cylindrical. In such a case, $R_{RG}^T = r_{c0}$ (r_c is the cloud cylindrical radius) can be significantly smaller than the length of the disrupted atmosphere, l_c (Ayal et al. 2000). The system of equations describing this case can be written as:

$$E_c = \frac{\pi l_c r_c^2 F_j}{(\hat{\gamma} - 1)c} \quad (17)$$

$$\frac{dr_c}{dt} = c_s = \left(\frac{\hat{\gamma}(\hat{\gamma} - 1)E_c}{M_c} \right)^{1/2} \quad (18)$$

$$\frac{d^2 z_c}{dt^2} = \frac{2l_c F_j r_c}{cM_c}. \quad (19)$$

Substituting Eq. (17) into Eq. (18), we obtain:

$$r_c(t) = r_{c0} e^{t/t_{ce}}. \quad (20)$$

As in the weak case, r_{c0} and t_{ce} are the initial radius and the expansion time of the cloud, where:

$$t_{ce} = \left(\frac{cM_c}{\pi \hat{\gamma} F_j l_c} \right)^{1/2} = 1 M_{c,28}^{1/2} F_{j,14}^{-1/2} l_{c,14}^{-1/2} \text{ day}, \quad (21)$$

with $l_{c,14} = (l_c/10^{14} \text{ cm})$ and $F_{j,14} = (F_j/10^{14} \text{ erg cm}^{-2} \text{ s}^{-1})$.

If we neglect the initial velocity of the cloud in the z -direction, the distance covered by the cloud is as follows:

$$z(t) - z_{jc} = \frac{2F_j l_c r_{c0} t_{ce}}{cM_c} \left(t_{ce} e^{t/t_{ce}} - t_{ce} - t \right), \quad (22)$$

with a velocity

$$v_z(t) = \frac{2F_j l_c r_{c0} t_{ce}}{cM_c} \left(e^{t/t_{ce}} - 1 \right). \quad (23)$$

As in the weak case, after substantial expansion equalizing cloud and jet pressures overestimates the energy transfer from the jet to the elongated cloud, and the relation $dE_c/dt \sim \pi r_c^2 F_j$ should be used. This phase is characterized by a slower, but still quite fast, power-law-like expansion rate.

3. RADIATION

Particles could be accelerated in the shocked jet region below the cloud. As noted in Sect. 1, the jet is probably magnetically dominated at $z \lesssim z_T$. Therefore, one can estimate the magnetic field in the jet as follows:

$$B_j \approx \sqrt{\frac{8L_j}{cz^2\theta^2}} \approx 200 L_{j,44}^{1/2} z_{16}^{-1} \theta_{-1}^{-1} \text{ G}, \quad (24)$$

where $L_{j,44} = L_j/10^{44} \text{ erg s}^{-1}$. The expected magnetic field in the shocked jet region should be also strong, probable of a similar strength to B_j . Under such a magnetic field, one can estimate the acceleration timescale:

$$t_{acc} = \frac{E}{\dot{E}_{acc}} \sim \frac{\xi E}{q B_j c} \approx 0.1 \xi E_2 B_{j,2}^{-1} \text{ s}, \quad (25)$$

where ξ is the acceleration efficiency parameter, q is the particle charge, $E_2 = E/10^2 \text{ TeV}$, and $B_{j,2} = B_j/10^2 \text{ G}$, the maximum energy of protons and electrons are

$$E_{p \text{ max}} \approx \sqrt{\frac{3}{2\xi}} q B_j r_c \approx 10^7 B_{j,2} r_{c,14} \xi^{-1/2} \text{ TeV} \quad (26)$$

and

$$E_{e \text{ max}} \approx \sqrt{\frac{qc}{\xi a_s B_j}} \approx 10 B_{j,2}^{-1/2} \xi^{-1/2} \text{ TeV}, \quad (27)$$

respectively, where $a_s = 1.6 \times 10^{-3}$. Equation (26) is obtained from limiting the proton acceleration by Bohm diffusion escape from the interaction region, of size

$r_{c,14} = (r_c/10^{14} \text{ cm})$, and Eq. (27) is obtained from limiting the electron acceleration through synchrotron cooling. Even taking a high $\xi \sim 10$ (for mildly relativistic shocks, as those of supernova explosions, $\xi \sim 10^4$), electron energies will be too low to explain the HESS spectrum of M87 up to energies of few 10 TeV (Aharonian et al. 2006), whereas protons may be accelerated up to ultra-high energies. In addition, the expected B_{jet} -values could easily suppress any IC component. We note that even for diffusion faster than Bohm, or under bigger ξ -values, protons could still reach enough energy to explain observations. On the other hand, the cloud density can be high, making of pp interactions the best candidate for gamma-ray production in the RG-jet scenario, the characteristic cooling time for pp collisions being:

$$t_{pp} \approx \frac{10^{15}}{n_c} = 10^5 n_{c,10}^{-1} \text{ s}, \quad (28)$$

where $n_{c,10} = n_c/10^{10} \text{ cm}^{-3}$ is the cloud density. We note that the high cloud density should not affect significantly the proton acceleration, which would occur in the far less dense jet shocked region. Nevertheless, protons should penetrate in the acceleration process and, in the Blandford-Znajek scenario of jet formation (Blandford & Znajek 1977; Beskin et al. 1992) the jet is probably formed only by pairs at z_{jc} . Therefore, some cloud material should penetrate into the shocked jet medium, which can occur through Rayleigh-Taylor instabilities (Chandrasekhar 1961; Imshennik 1972). We present in Fig. 2 a sketch of the mixing, proton acceleration and gamma-ray production processes. We do not specify here the physics of particle acceleration, although this could take place by one or a combination of different mechanisms: magnetic reconnection right after the shock in the jet, shear acceleration due to the strong velocity gradients close to the contact discontinuity, or some sort of stochastic acceleration due to magnetic turbulence downstream the jet shock. Regarding other proton radiation mechanisms, proton synchrotron will not be efficient in our case, with $t_{p \text{ sync}} \approx 5 \times 10^{10} B_{j,2}^{-2} \text{ s} \gg t_{pp}$. Also photomeson production can be also neglected, since $t_{p\gamma} \sim 5 \times 10^6 L_{41} r_{c,14}^{-1} \epsilon_{\text{keV}}^{-1} \text{ s} \gg t_{pp}$, where $L_{41} = (L/10^{41} \text{ erg s}^{-1})$ and $\epsilon_{\text{keV}} = (\epsilon/1 \text{ keV})$ would be the luminosity produced in the region and the ambient photon energy (e.g. thermal X-rays; see below), respectively. photomeson production with keV ambient photons would require protons with energies above $\sim 100 \text{ TeV}$.

Hereafter, we will treat the generation of protons with energies $> 100 \text{ GeV}$ phenomenologically, assuming that a fraction η of the total eclipsed jet luminosity is converted to relativistic protons: $L_p = \eta \pi r_c^2 F_j$. We also assume that these protons can effectively reach the cloud, where they suffer pp interactions that lead to π^0 -meson production, although some of them could escape surrounding the cloud. Once in the cloud, protons can be effectively trapped during the RG-jet interaction time for magnetic fields as low as few G, since:

$$B_c = \frac{t E c}{3 q r_c^2} \approx 0.03 t_5 E_2 r_{c,14}^{-2} \text{ G}, \quad (29)$$

where $t_5 = t/10^5 \text{ s}$ is the time inside the cloud. Note that Eq. (29) has been derived assuming Bohm diffusion,

but faster diffusion regimes would still allow to keep protons trapped in the cloud.

The typical fraction of the proton energy transferred per collision to the leading gamma rays is $E_\gamma = 0.17E_p$ (Kelner et al. 2006) in the optically thin case, and around twice that value for optically thick media neglecting gamma-rays from other secondary particles. Therefore, we can characterize the proton-gamma ray energy transfer by

$$\chi \equiv E_\gamma/E_p = 0.17[2 - \exp(-t/t_{pp})]. \quad (30)$$

Two phases of the cloud expansion can be distinguished: the radiatively efficient regime, i.e. with $\chi \approx 0.34$ or $t > t_{pp}$, and the radiatively inefficient regime, with $\chi = 0.17$ or $t < t_{pp}$. Thus, from the simplifications above, the gamma-ray luminosity in the pp optically-thick case can be written as:

$$L_\gamma \approx 0.34\eta\pi r_c^2 F_j, \quad (31)$$

where is seen that $L_\gamma \propto r_c^2$. In the pp optically thin case, only a fraction t/t_{pp} of L_p is lost through pp collisions, and $L_\gamma \propto r_c^{-1}$. The general expression for the gamma-ray luminosity during a RG-jet interaction event becomes:

$$L_\gamma \approx \pi\eta\chi r_c^2 F_j (1 - \exp(-t/t_{pp})). \quad (32)$$

Given the fast expansion of the cloud, either in the spherical or the elongated case, one can expect a sharp spike in the light curve.

Secondary electrons and positrons (e^\pm), injected by pp collisions with an energy rate $\sim L_\gamma$, could emit most of their energy through synchrotron radiation. Given the moderate energy budget, the radio, optical and X-ray fluxes would be below the observed values in the region of interest. However, at later times, conditions may change becoming more suitable for radio emission. Thus, it cannot be discarded that RG-jet interactions could eventually have a low-energy faint counterpart produced by secondary or thermal e^\pm , or even by a primary population of accelerated electrons.

The gamma-ray pp light curve for M87 is presented in Fig. 4, in which the maximum is reached at $t_{\text{peak}} \approx 4 \times 10^5$ s, with a width of $\sim 1 - 2$ days. A value for η of 0.1 has been adopted. We recall that our approach is valid for $t < t_t \approx 4.7 \times 10^5$ s (see Sect. 2), hence the adopted cloud evolution model describes the gamma-ray peak properly. We show the gamma-ray lightcurve for the weak tidal disruption case as the most conservative scenario. In the strong tidal disruption case, the lightcurve would be similar but the gamma-ray maximum would be even higher.

3.1. Optimal radiation case

Around the gamma-ray maximum, at $t \sim t_{\text{peak}}$, and because of $t_{\text{peak}} \sim t_{pp}$, one can measure the cloud density and radius n_{cp} and r_{cp} . From

$$n_{cp} = \frac{3M_c}{4\pi m_p r_{cp}^3}; \quad (33)$$

plus the variability time:

$$t_v \approx t_{pp} \approx \frac{10^{15}}{n_{cp}} \quad (34)$$

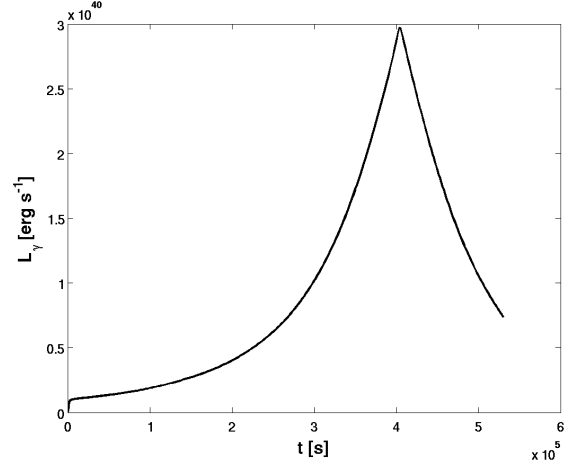


FIG. 4.— Gamma-ray pp lightcurve for the weak tidal disruption case. The same parameter values as in Fig. 3 have been adopted.

one can determine

$$r_{cp} = \left(\frac{3M_c t_v}{4\pi 10^{15} m_p} \right)^{1/3}. \quad (35)$$

We can characterize the variability time t_v , which would correspond to the characteristic duration of the gamma-ray peak, as follows:

$$t_v = 2 \frac{L_\gamma}{dL_\gamma/dt} = \frac{t_{ce}(1 - t_{\text{peak}}/t_{ce})}{2}. \quad (36)$$

The condition $r = r_{cp}$, and Eqs. (9), (35) and (36), allow the derivation of the following expression:

$$\left(\frac{48M_c}{\pi 10^{15} m_p} \right)^{1/3} t_v^{7/3} = t_{ce}^2 r_{c0}. \quad (37)$$

Then, from Eq. (37), and assuming $t_{ce} = t_{jc}$, $(1 - t_{\text{peak}}/t_{ce}) \ll 1$ and $r_{c0} = R_{RG}^T$, one obtains:

$$t_{ce} = \frac{L_j^{3/20} \hat{\gamma}^{3/20} \theta^{1/10} t_v^{21/20}}{50 \times 10^{1/4} \pi^{3/20} c^{3/20} G^{1/5} M_{BH}^{1/10} m_p^{3/20} M_{RG}^{1/10}} \quad (38)$$

$$M_c = \left(\frac{L_j^6 \hat{\gamma}^6 M_{RG}^7 t_v^7}{750^5 \pi^6 G^3 M_{BH}^4 m_p \theta^6} \right)^{1/5} \quad (39)$$

$$z_{jc} = \left(\frac{M_{BH}^4 G^3 L_j^{3/2} \hat{\gamma}^{3/2} t_v^{21/2}}{3.16 \times 10^{22} \pi^{3/2} m_p^{3/2} c^{3/2} M_{RG} \theta^9} \right)^{1/15}. \quad (40)$$

Finally, substituting (3), (4), (35) and (39) into (31), the expression for the gamma-ray luminosity around the lightcurve peak can be derived:

$$L_\gamma = \frac{\eta\chi}{10^9 \pi^{3/5}} \left(\frac{M_{RG}}{M_{BH}^4} \right)^{4/15} \left(\frac{\hat{\gamma}^3 L_j^8 t_v}{c^3 G^4 m_p^3 \theta^8} \right)^{1/5} \\ \approx 8 \times 10^{40} \eta_{-1} L_{j,44}^{8/5} t_{v,5}^{1/5} M_{RG}^{4/15} M_{BH,9}^{-16/15} \theta_{-1}^{-8/5} \text{ erg s} \quad (41)$$

where $M_{BH,9} = (M_{BH}/10^9 M_\odot)$, $\eta_{-1} = \eta/0.1$ and $t_{v,5} = (t_v/10^5 \text{ s})$. Adopting typical parameter values for M87, $L_j = 2 \times 10^{44} \text{ erg s}^{-1}$, $M_{BH} = 6.4 \times 10^9 M_\odot$, $\theta_{-1} = 1$, $t_v = 2 \times 10^5$ days, $M_{RG} = 1 M_\odot$, $z_{jc} \approx 3.6 \times 10^{16} \text{ cm}$, $M_c \approx$

1.4×10^{28} gr, and $\eta_{-1} = 1$, one gets $L_\gamma \approx 4 \times 10^{40}$ erg s $^{-1}$, in good agreement with observations (Aharonian et al. 2006; Albert et al. 2008; Acciari et al. 2009, 2010). We remark that the t_v -value would be in agreement with the observed event durations.

3.2. Thermal radiation of the cloud and self- $\gamma\gamma$ absorption

In the case of M87, near the peak of the very high-energy (VHE) radiation, i.e. $n_{\text{cp}} \approx 10^{10}$ cm $^{-3}$ and $r_{\text{cp}} \approx 10^{14}$ cm, the cloud is optically thin to the radiation produced by its own shocked plasma:

$$\tau_{e\gamma} = r_{\text{cp}} n_{\text{cp}} \sigma_T \approx 0.6 < 1, \quad (42)$$

where $\sigma_T = 6.65 \times 10^{-25}$ cm $^{-2}$ is the Thompson cross section. At the temperature of the shocked cloud, $T_c \sim 10^{10}$ K, the timescales for Coulombian thermalization through $p-p$ and $e-e$ scattering are $t_{e-e} \approx t_{p-p} \approx T_8^{3/2} n_{c10}^{-1} \approx 1000$ s ($t_{ep} \approx 10^3 T_8^{3/2} n_{c10}^{-1} \approx 10^6$ s for $p-e$ scattering). Therefore, the shocked cloud is thermalized.

The main channel of thermal radiation is free-free emission, with a photon mean energy $\langle \epsilon \rangle \sim kT_c \sim 1$ MeV and total luminosity (Berestetskii et al. 1971; Kaplan & Pikel'Ner 1979):

$$L_X = 2.1 \times 10^{-27} T^{1/2} n_c^2 V_{\text{cp}} \approx 10^{41} \text{ erg s}^{-1}, \quad (43)$$

where $V_{\text{cp}} = 4\pi r_{\text{cp}}^3/3$. The concentration of thermal photons can be estimated as

$$n_X = \frac{L_X}{4\pi c k T_c r_{\text{cp}}^2} \approx 2 \times 10^7 \text{ cm}^{-3}, \quad (44)$$

yielding an optical depth for photon-photon absorption at the energy of the strongest attenuation ($\sim m_e^2 c^4 / \langle \epsilon \rangle$): $\tau_{\gamma\gamma} \sim 0.2 n_X r_{\text{cp}} \sigma_T \approx 10^{-3} \ll 1$ (Aharonian 2004), being much smaller at 1 TeV. The free-free radiation should not show any thermal lines, presenting a very hard non-thermal X-ray spectrum.

For very powerful jets the condition presented in Eq. (42) is not fulfilled, the shocked plasma is radiation dominated and cooler, and Eqs. (43) and (44) do not apply. The cloud is then optically thick, with the radiation being a black body with mean energy of photons $\langle \epsilon \rangle \approx 3kT_b \approx 10 L_{j,44}^{1/5} M_{\text{BH},9}^{-2/15} t_{v,5}^{-21/60}$ eV. The optical depth for gamma-rays is $\tau_{\gamma\gamma} \approx 10^4 L_{j,44}^{3/5} M_{\text{BH},9}^{1/15} t_{v,5}^{-26/15}$, with the radiation being suppressed for energies $E_{\text{th}} \gtrsim m_e^2 c^4 / 3kT_b \sim 50$ GeV, where m_e is the electron mass. Photon-photon absorption creates pairs with energies $\gtrsim E_{\text{th}}$ that cool down through synchrotron emission with spectral energy distribution $\epsilon F_\epsilon \propto \epsilon^{1/2}$ below 10 keV, with the higher energy part of the spectrum softer, reaching MeV-GeV energies. Under $\tau_{\gamma\gamma} > 1$ and reasonable magnetic fields, the synchrotron luminosity will be similar to the absorbed gamma-ray luminosity.

The X-ray flare detected from M87 almost simultaneously with the VHE flare (see, e.g., Acciari et al. 2009) may have been also produced at the RG-jet interaction. This X-ray flare could be of synchrotron nature, with possible contributions from a primary electron component, secondary e^\pm from pp and photon-photon interactions, and thermal free-free radiation. Regardless the

origin, the observed X-ray emission could have a counterpart at lower energies. If it came from the region of gamma-ray production, the spectrum should be quite hard to avoid too many optical photons that would lead otherwise to significant TeV photon absorption. Optical observations simultaneous with a gamma-ray flare could clarify this point.

4. DISCUSSION AND CONCLUSIONS

The total jet luminosity can be inferred from observations using Eq. (41):

$$L_j = 8 \times 10^{44} L_{\gamma,41}^{5/8} M_{\text{BH},9}^{2/3} \theta_{-1} \eta_{-1}^{-5/8} t_{v,5}^{-1/8} M_{\text{RG}}^{-1/6} \text{ erg s}^{-1}. \quad (45)$$

This formula weakly depends on the observables, being almost insensitive to M_{RG} , on the other hand hard to estimate. This provides therefore a quite robust estimate of the jet luminosity with η as most unknown parameter. Actually, if L_j were known, then η could be also estimated.

For the most powerful jets, L_γ would be limited by the jet size becoming $L_\gamma = \chi \eta L_j$. Taking for instance $L_j \sim 10^{47}$ erg s $^{-1}$, L_γ could be as high as $\approx 2 \times 10^{45} \eta_{-1}$ erg s $^{-1}$. An improvement of a factor of several in the VHE sensitivity (e.g. through the forthcoming the Cherenkov Telescope Array -CTA-) would test our gamma-ray predictions for the whole RG-jet interaction process, including the early cloud expansion phase, allowing for a detailed study of the involved (magneto)hydrodynamics, particle acceleration, and radiation.

We remark that, if a detectable gamma-ray flare with a duration of few days were to be produced in M87, in particular through pp interactions, the cloud should have a mass of $\sim 10^{28}$ g. Such a massive cloud cannot acquire a large speed in the jet direction at the times when pp collisions are an efficient gamma-ray emitting mechanism, and therefore the emission will not suffer significant Doppler boosting. In the case of a lighter cloud, large Lorentz factors can be achieved, but then pp interactions will be inefficient producing gamma-rays, the probability to detect a flare lower due to beaming, and the duration of the event shorter than observed because of faster expansion and beaming.

Coming back to the question of cloud mass, we note that to extract a cloud with a mass $> 10^{28}$ g, a more powerful jet than in M87, for similar jet-RG interaction conditions, would be required (see Eq.(39)).

An important question is whether there are enough RGs in M87 at the relevant jet scales. The model presented here would require few interactions per year to explain the observations in M87. Since the typical duration of the RG-jet interaction is of about 3–4 days, the RG filling factor should be $\Upsilon \sim 4/365 \approx 10^{-2}$. With a jet volume at the relevant scales of $\sim \pi \theta^2 z_T^3/3$, the density of RGs in the region should be $\sim \Upsilon/V \sim 2 \times 10^6$ pc $^{-3}$ for M87. Unfortunately, no direct information is available on the density of stars in the vicinity of the SMBH in M87. The stellar mass in a sphere with a radius of 80 pc is estimated in $2 \times 10^8 M_\odot$ (e.g. Gebhardt & Thomas 2009), and these observational data should be extrapolated four orders of magnitude down to ~ 0.01 pc. Thus, depending on the assumed extrapolation law, the num-

ber of RGs in the vicinity of the SMBH may or may not be enough. It is worth noting that a dense stellar cluster near the SMBH could be behind the broad-line region in AGN as produced by the blown-up atmosphere of red dwarfs, which would imply the presence of numerous RGs in the center of AGN (Penston 1988). In addition, studies of the possible stellar density profiles in the vicinity of the SMBH in AGN (Bisnovatyi-Kogan et al. 1982; Murphy et al. 1991) show that densities like the required one ($\sim 2 \times 10^6 \text{ pc}^{-3}$) could be achieved. The observation of VHE flares could be already an indication that enough RGs are present near the SMBH in M87.

Interestingly, RG/jet interactions are expected to be transient phenomena. At higher jet heights, although many RGs could be simultaneously present in the jet rendering rather continuous emission, the much more diluted jet would not remove a significant amount of material from the star and the effective cross section of the interaction would be just R_{RG} , yielding a low energy budget for such a multiple interaction events.

The scenario presented here, adopted to explain the day VHE flares observed from M87, could also be relevant in other non-blazar AGN. For blazar sources the beamed emission would overcome the RG-jet interaction, expected to be weakly beamed due to moderate v_z -values. For instance, the closest AGN, the radio galaxy Cen A, at ~ 3.8 Mpc distance (Rejkuba 2004), could also show detectable flare like emission. At present, persistent faint VHE emission has been detected (Aharonian et al. 2009) with $L_\gamma = 2.6 \times 10^{39} \text{ erg s}^{-1}$. Accounting for the black hole mass of this AGN, $M_{\text{BH}} = 5.5 \times 10^7 M_\odot$, taking the observed VHE luminosity as a reference, and assuming $t_v \sim 1$ day, one derives implementing Eq. 45 a jet luminosity $L_j = 1.2 \times 10^{42} \text{ erg s}^{-1}$, a rather modest value. Therefore, it cannot be excluded that RG-jet

interactions may contribute to the VHE radiation detected from Cen A, or that transient activity due to RG-jet interactions may be observed from this source. Another case, the radio galaxy NGC1275, at a distance of 73 Mpc (Hicken et al. 2009), shows variable behaviour in GeV (Abdo et al. 2009). The GeV luminosity is of about $2 \times 10^{43} \text{ erg s}^{-1}$. Using Eq. (45), we can estimate the power of the jet as $5 \times 10^{44} \text{ erg s}^{-1}$ adopting an $M_{\text{BH}} = 10^8 M_\odot$. In the case of NGC 1275 the shocked cloud would be optically thick at the luminosity peak, implying significant attenuation of the TeV emission through photon-photon absorption with a cutoff around 50 GeV.

At farther distances, the strong jet luminosity dependence $L_\gamma \propto L_j^{1.6}$ implies that FR II sources with say $L_j \sim 10^{46} \text{ erg s}^{-1}$ may be still detectable up to distances of ~ 0.5 Gpc (internal absorption should be included in these cases; see Aharonian et al. 2008). Also, the luminosity in the range 0.1–100 GeV would also be significant unless there is a strong low-energy cutoff in the proton spectrum. Therefore, Fermi may detect day-long GeV flares originated due to RG-jet interactions from FR II galaxies up to distances of few 100 Mpc. Summarizing, GeV and TeV instrumentation can potentially detect a number of RG-jet interactions per year taking place in nearby FR II and very nearby FR I galaxies, with the most powerful events being detectable up to 1 Gpc.

ACKNOWLEDGMENTS

V.B-R. wants to thank A. T. Araudo and G. E. Romero for fruitful discussions. V.B-R. acknowledges support by the Ministerio de Educación y Ciencia (Spain) under grant AYA 2007-68034-C03-01, FEDER funds. V.B-R. thanks Max Planck Institut fuer Kernphysik for its kind hospitality and support.

REFERENCES

- Abdo, A. A., et al. 2009, ApJ, 699, 31
 Acciari, V. A., et al. 2009, Science, 325, 444
 —. 2010, ArXiv e-prints
 Aharonian, F., et al. 2006, Science, 314, 1424
 —. 2009, ApJ, 695, L40
 Aharonian, F. A. 2000, New Astronomy, 5, 377
 —. 2002, MNRAS, 332, 215
 —. 2004, Very high energy cosmic gamma radiation : a crucial window on the extreme Universe, ed. Aharonian, F. A.
 Aharonian, F. A., Khangulyan, D., & Costamante, L. 2008, MNRAS, 387, 1206
 Albert, J., et al. 2008, ApJ, 685, L23
 Araudo, A. T., Bosch-Ramon, V., & Romero, G. E. 2010, A&A, in press [astro-ph/]
 Ayal, S., Livio, M., & Piran, T. 2000, ApJ, 545, 772
 Barkov, M. V., & Komissarov, S. S. 2008, International Journal of Modern Physics D, 17, 1669
 Bednarek, W., & Protheroe, R. J. 1997, MNRAS, 287, L9
 Begelman, M. C., Blandford, R. D., & Rees, M. J. 1984, Reviews of Modern Physics, 56, 255
 Berestetskii, V. B., Lifshitz, E. M., & Pitaevskii, V. B. 1971, Relativistic quantum theory. Pt.1, ed. Berestetskii, V. B., Lifshitz, E. M., & Pitaevskii, V. B.
 Beskin, V. S., Istomin, Y. N., & Pared, V. I. 1992, Soviet Astronomy, 36, 642
 Bisnovatyi-Kogan, G. S., & Blinnikov, S. I. 1977, *ĭp*, 59, 111
 Bisnovatyi-Kogan, G. S., Churaev, R. S., & Kolosov, B. I. 1982, *ĭp*, 113, 179
 Blandford, R. D., & Znajek, R. L. 1977, MNRAS, 179, 433
 Chandrasekhar, S. 1961, Hydrodynamic and hydromagnetic stability, ed. Chandrasekhar, S.
 Dar, A., & Laor, A. 1997, ApJ, 478, L5+
 Diener, P., Frolov, V. P., Khokhlov, A. M., Novikov, I. D., & Pethick, C. J. 1997, ApJ, 479, 164
 Gebhardt, K., & Thomas, J. 2009, ApJ, 700, 1690
 Ghisellini, G., Maraschi, L., & Treves, A. 1985, *ĭp*, 146, 204
 Hicken, M., Wood-Vasey, W. M., Blondin, S., Challis, P., Jha, S., Kelly, P. L., Rest, A., & Kirshner, R. P. 2009, ApJ, 700, 1097
 Imshennik, V. S. 1972, Soviet Physics Doklady, 17, 576
 Ivanov, P. B., Chernyakova, M. A., & Novikov, I. D. 2003, MNRAS, 338, 147
 Junor, W., Biretta, J. A., & Livio, M. 1999, Nature, 401, 891
 Kaplan, S. A., & Pikel'Ner, S. B. 1979, Fizika mezhzvezdnoi sredy, ed. Kaplan, S. A. & Pikel'Ner, S. B.
 Kelner, S. R., Aharonian, F. A., & Bugayov, V. V. 2006, Phys. Rev. D, 74, 034018
 Khokhlov, A., Novikov, I. D., & Pethick, C. J. 1993a, ApJ, 418, 181
 —. 1993b, ApJ, 418, 163
 Komissarov, S. S., Barkov, M. V., Vlahakis, N., & Königl, A. 2007, MNRAS, 380, 51
 Liang, E. P. T., & Thompson, K. A. 1979, MNRAS, 189, 421
 Lodato, G., King, A. R., & Pringle, J. E. 2009, MNRAS, 392, 332
 Mannheim, K. 1993, *ĭp*, 269, 67
 Mücke, A., & Protheroe, R. J. 2001, Astroparticle Physics, 15, 121
 Murphy, B. W., Cohn, H. N., & Durisen, R. H. 1991, ApJ, 370, 60
 Neronov, A., & Aharonian, F. A. 2007, ApJ, 671, 85
 Owen, F. N., Eilek, J. A., & Kassim, N. E. 2000, ApJ, 543, 611
 Penston, M. V. 1988, MNRAS, 233, 601
 Rejkuba, M. 2004, *ĭp*, 413, 903
 Rieger, F. M., & Aharonian, F. A. 2008, *ĭp*, 479, L5

Rieger, F. M., Bosch-Ramon, V., & Duffy, P. 2007, *Ap&SS*, 309,
119
Schopper, R., Lesch, H., & Birk, G. T. 1998, *âp*, 335, 26

Shakura, N. I. 1972, *AZh*, 49, 921
Shakura, N. I., & Sunyaev, R. A. 1973, *âp*, 24, 337